CHEMICAL ENGINEERING TRANSACTIONS
VOL. 99, 2023
A publication of AIDIC
The Italian Association of Chemical Engineering
Online at www.cetjournal.it
Guest Editors: Sauro Pierucci, Flavio Manenti

ISBN 978-88-95608-98-3; **ISSN** 2283-9216
DOI: 10.3303/CET2399051

Preliminary Assessment of Copper/Cerium Mixed Oxides for Thermochemical Energy Storage Applications

Gianluca Landi[a], Claudio Tregambi[ab]*, Piero Bareschino[b], Erasmo Mancusi[b], Francesco Pepe[b], Roberto Solimene[a]

[a] Istituto di Scienze e Tecnologie per l'Energia e la Mobilità Sostenibili, CNR, Piazzale Tecchio 80, 80125 Napoli, Italia
[b] Dipartimento di Ingegneria, Università degli Studi del Sannio, Piazza Roma 21, 82100 Benevento, Italia
claudio.tregambi@unisannio.it

An extensive exploitation of renewable energies is required to face climate change, and reduce the dependence on fossil fuels. Thermochemical energy storage (TCES) systems are bound to play a major role in the next years to overcome the intrinsic variability of many renewable sources, thus increasing their dispatchability. Within this field, reversible gas-solid chemical reactions are among the most promising systems thanks to high theoretical values of energy storage density, and virtual unlimited time scales of energy storage. Copper oxide is an interesting candidate for TCES, but suffers from particle sintering/agglomeration at the high process temperature required by the system. In this work, several Cu:Ce mixed oxides have been synthesized and tested in a thermogravimetric analyzer under process parameters relevant to TCES applications, with the aim of preventing copper oxide sintering/agglomeration. Morphology and chemical composition of the synthesized and reacted samples have been scrutinized by means of XRD and SEM-EDS analyses.

1. Introduction

The current environmental, social, and economic scenario demands relevant modifications to the national energy plan of several Countries. The development of efficient energy storage systems is under the spotlight to deal with the intrinsic intermittence of renewable energies. Conversion of renewable energy into fuels that can be used when necessary is a possible strategy. This can be achieved through integration with carbon capture technologies (Tregambi et al., 2022), gasification processes (Bareschino et al., 2021), H_2O/CO_2 thermochemical splitting (Portarapillo et al., 2019, 2022) or solar reforming of CH_4 streams (Padula et al., 2022). Another solution is the use of thermochemical energy storage (TCES) systems based on reversible chemical reactions: collection of renewable energy occurs through the endothermal reaction step, while reversal of the reaction allows the release of the stored energy. Decomposition and recombination of metal hydroxides, carbonates, oxides are among the most investigated systems (Carrillo et al., 2019). Copper oxide is an interesting material for TCES thanks to its high theoretical energy storage density and to the wide availability and low toxicity of the material. The endothermic reduction of cupric oxide (CuO) to cuprous oxide (Cu_2O) can be performed in N_2 or air, while the exothermic re-oxidation is typically performed in air. The reaction temperature ranges within 700–1100 °C according to different literature studies. One of the main drawbacks of copper oxides is the strong decay of reactivity over cycling induced by the material sintering/agglomeration, as the melting temperature of Cu_2O (~1200 °C) is quite close to the reaction temperature. Different strategies are investigated in literature to overcome this drawback. The use of rotary kiln to decrease particle sintering/agglomeration has been considered (Alonso et al., 2015). The synthesis of mixed or supported copper oxides is another investigated solution. On this topic, Block and Schmücker (2016) tested several copper binary oxides (Co, Mn, Fe, Cr), finding that Cu/Co mixed oxides are promising as TCES material, thanks to high reaction kinetics and enthalpy. Gigantino et al. (2020) tested CuO mixed with YSZ, and reported a good sintering resistance over repeated cycles. Xiang et al. (2021) tested Al-doped copper oxides, and stated that the formation of a mixed phase ($CuAl_2O_4$) prevented material sintering. In the present work, the use of CuO doped with ceria is experimentally investigated.

Paper Received: 20 December 2022; Revised: 19 March 2023; Accepted: 22 April 2023
Please cite this article as: Landi G., Tregambi C., Bareschino P., Mancusi E., Pepe F., Solimene R., 2023, Preliminary Assessment of Copper/cerium Mixed Oxides for Thermochemical Energy Storage Applications, Chemical Engineering Transactions, 99, 301-306 DOI:10.3303/CET2399051

Literature studies on this system mostly dealt with chemical looping combustion (Hedayati et al., 2012; Rydén et al., 2014). Here, TCES is considered, that is characterized by different process conditions. The use of a Cu-Ce system for TCES was recently investigated by Yilmaz et al. (2020), using a CuO content of 40%$_{wt}$ and a reactive atmosphere of 5%$_v$ O_2. In the present study, samples with a different Ce:Cu ratio were synthesized. The reactivity of the materials was then investigated by performing the reduction step in N_2 and the oxidation step in air, using a thermogravimetric analyzer with simultaneous thermal analysis. Reaction degree and materials stability over iterated cycling were evaluated. Samples were analyzed by means of X-ray Diffraction (XRD) and Scanning Electron Microscopy (SEM) to scrutinize the phases formed and the morphology of the materials. Finally, the attainable densities of energy storage were computed to assess the potentiality of these materials towards TCES applications.

2. Experimental

Four different samples were synthesized and tested in the present experimental campaign, with nominal composition detailed in Table 1. In any case, the following experimental procedure was used. Appropriate amounts of cerium (III) nitrate hexahydrate and copper (II) nitrate hemi(pentahydrate), purchased from Sigma-Aldrich and used as received, were dissolved in bi-distillate water. Then, the solution was dried in a thermostatic stove at 120°C. The sample was then calcined at 950 °C in a muffle furnace under air for 5 h.

Table 1: Nominal mass and atomic composition of the four synthesized samples

Name	CuO:CeO_2 mass ratio	Cu:Ce atomic ratio	Surface Cu:Ce atomic ratio	
			(as prepared)	(4 cycles)
Cu100	100:0	1.00	–	–
Cu70	70:30	0.83	45.1	5.2
Cu40	40:60	0.59	38.1	7.8
Cu0	0:100	0.00	–	–

The materials were then tested in a thermogravimetric analyzer with simultaneous thermal analysis (Mettler Toledo TGA/DSC 3$^+$) to measure the mass loss/gain of the samples over iterated reduction/oxidation cycles, together with the heat absorbed and released by the samples during the chemical reactions. Reduction was performed using N_2 and oxidation using synthetic air, both with 99.999% purity. The temperature was instead fixed to 950 °C for both reaction steps. During a typical test, a sample of about 30–40 mg was placed in a 90 µL Al_2O_3 crucible and heated to 950 °C at 20 °C min^{-1} under a N_2 flow of 50 mL min^{-1}. Then, nine isothermal steps at 950°C, 50 min each, were performed by switching the gas atmosphere between N_2 and synthetic air, respectively. The flow stream was always set at 50 mL min^{-1}. The last isothermal step, as well as the final cooling of the sample to ambient temperature, were performed in N_2 to recover the samples in their reduced state. For each reaction step, it was computed the mass loss/gain with respect to the previous step as:

$$\Delta m = \frac{m_N - m_{N-1}}{m_{N-1}} \quad (1)$$

where N is a counter for the step (N = 1…9) and m is the mass of the sample at the end of the relevant reaction step. Depending on the step considered, Δm values may refer to the reduction or oxidation step. The integral heat flow signals associated with each reaction step were instead normalized to the mass of the reduced sample. Samples after the calcination in the muffle furnace, and after the thermogravimetric experiments, were analyzed by means of XRD and SEM with energy dispersive spectroscopy (SEM-EDS).

3. Results

3.1 Thermogravimetric analysis

Figure 1-a shows the thermogravimetric curves obtained for the different types of sample. In each case, the reference mass (m_{ref}) is that measured at about 700 °C during the initial heating, namely before the reduction step starts, but after the dehumidification and release of possible adsorbed compounds. The analysis of Figure 1-a reveals that Cu100, Cu70 and Cu40 undergo repeated reduction and oxidation reactions when the gaseous atmosphere changes from N_2 to air and vice-versa. Cu100 shows the highest mass reduction, followed by Cu70 and Cu40. Moreover, no decrease in reactivity is observed over the four performed cycles, as the mass loss and gain appear to be mostly constant over cycling for all the materials. Differently, for Cu0 (i.e., pure CeO_2), the mass variation upon O_2 concentration swing is almost null. Figure 1-b shows the mass loss and gain for all the samples, computed as from Eq. (1), together with the theoretical prediction values. The latter were

computed by assuming that all the cupric oxide reduces to cuprous oxide, while the ceria remains unchanged. Data in Figure 1-b confirm the stability of the samples over cycling, as *Δm* values for both reduction and oxidation steps are mostly constant over cycling. For Cu100, the experimental data are in good agreement also with the theoretical values, suggesting that the reduction of cupric oxide stops at cuprous oxide and does not proceed to metallic copper. For Cu70 and Cu40, the experimental values are higher than the theoretical ones, with a difference that is more pronounced for the sample richer in ceric oxide (Cu40). This difference could be ascribed to a composition of the samples being different from the nominal values reported in Table 1, or, alternatively, to a stronger reduction of the samples. The latter could be due to the reduction of a fraction of cuprous oxide to metallic copper and/or the reduction of a part of cerium oxide, both promoted by interfacial Cu:Ce interactions (Chen et al., 2015; Di Benedetto et al. 2017). It is worth noting that cerium oxide reduction can occur without the loss of its fluorite structure, i.e. with the formation of a non-stoichiometric $CeO_{2-\delta}$ phase (Portarapillo et al., 2022).

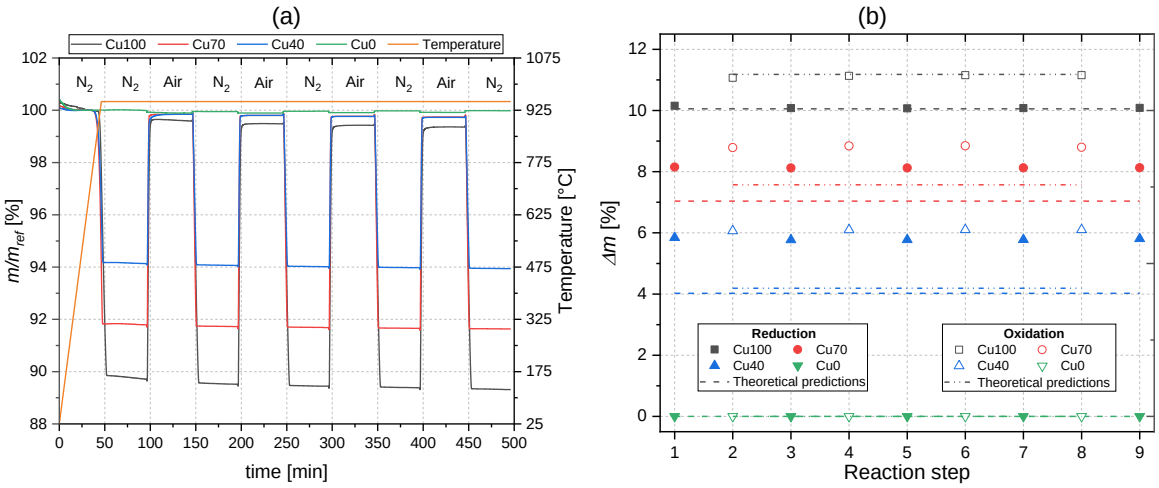

Figure 1: Thermogravimetric curves (a) and reduction/oxidation (b) extent of the four samples

3.2 XRD and SEM-EDS characterization

In the following, calcined samples before being tested will be labeled “as prepared”; samples that underwent the reduction-oxidation cycles as described in Section 3.1 will be labeled “4 cycles”. It is worth noting that the last treatment of the “4 cycles” procedure was a reduction.

Figure 2a shows the XRD spectra of the “as prepared” and “4 cycles” samples. As expected, Cu0, i.e. pure ceria, exhibits the typical fluorite structure spectrum and no differences can be detected before and after the reduction-oxidation cycles. ”As prepared” Cu100 shows a spectrum typical of the CuO tenorite structure, while Cu_2O is the only phase detected after the 4 reduction-oxidation cycles. These results agree with the thermogravimetric analysis. “As prepared” mixed samples show the signals of all phases identified on the pure samples. As expected, increasing the ceria content increases the relative ratio between CuO and CeO_2 peak intensity. In “4 cycles” samples the detected phases are Cu_2O and CeO_2, no peak related to metallic copper and/or Ce_2O_3 appearing. Actually, TGA results suggest an over-reduction of these samples, as stated in Section 3.1. In similar materials, the formation of metallic copper was not detected (Colussi et al., 2014; Imtiaz et al., 2015, 2021), also due to favorable thermodynamics (De Vos et al., 2020). However, as reported above, copper-ceria interfaces show unique redox features (Szabová et al., 2013; Popescu et al., 2017; Chen et al., 2019). In particular, interfacial copper-ceria sites can be reduced according to the following reaction:

$$Cu^{2+} - O^{2-} - Ce^{4+} \leftrightarrow Cu^{+} - \square - Ce^{3+} + \frac{1}{2}O_2$$

explaining both the absence of metallic copper and the over-reduction that increases by increasing the ceria content.

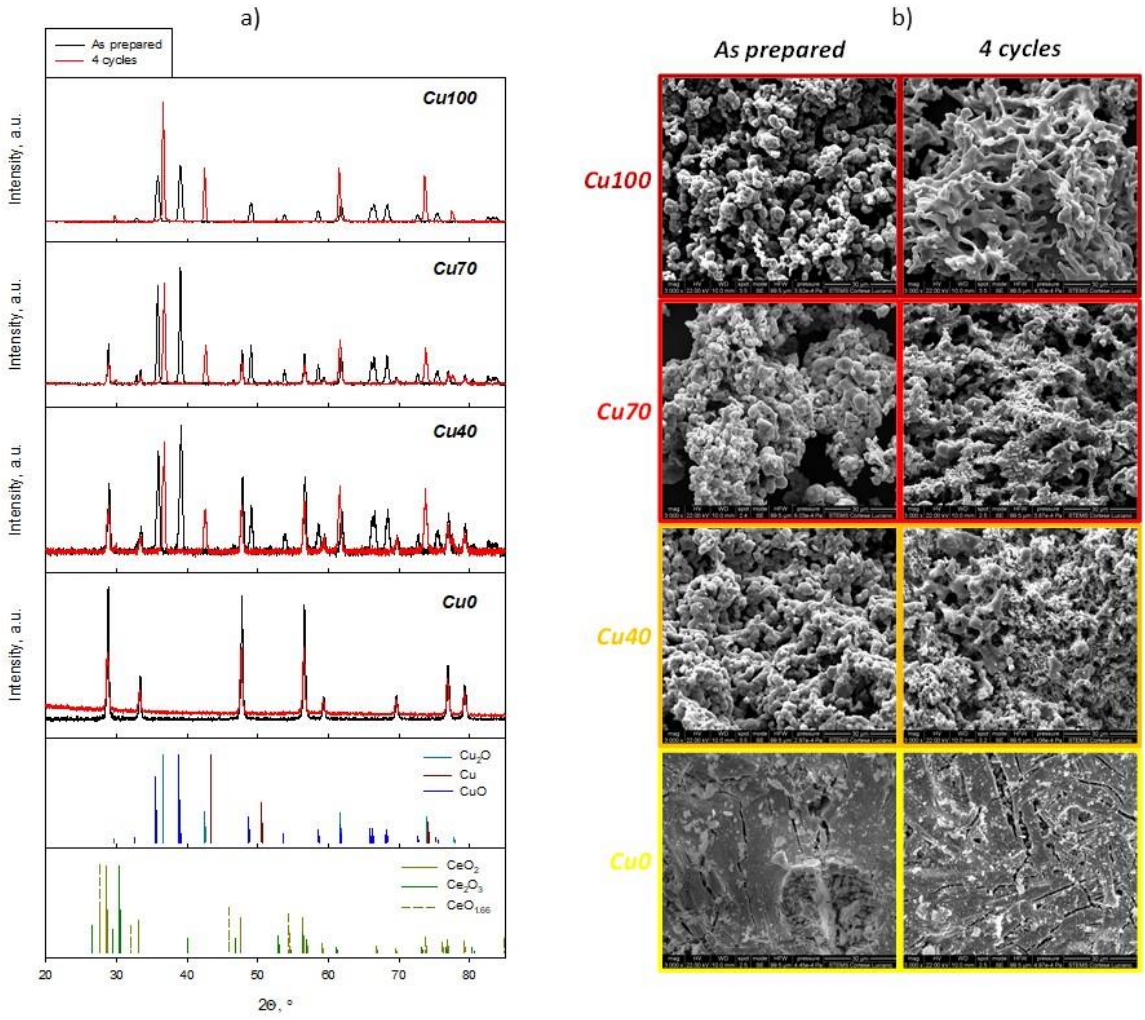

Figure 2: XRD (a) and SEM-EDS (b) of "as prepared" and "4 cycle" samples

Figure 2b shows SEM images and corresponding EDS analyses of "as prepared" and "4 cycles" samples. "As prepared" Cu100 and Cu0 show very different morphologies. Interestingly, the mixed samples appear more similar to Cu100. Table 1 shows the atomic ratio measured on the surface of the samples via EDS. The fresh samples show a very high Cu:Ce ratio, suggesting that copper oxide and cerium oxide form a core-shell structure, where cerium oxide particles are covered by copper oxide, as reported in Imtiaz et al. (2021). This would also account for the morphological similarity between the mixed samples and Cu100. As regards the samples after 4 cycles, the SEM images show a significant morphological restructuring (obviously excluding the Cu0 sample). In this restructuring, the cerium migrates towards the surface, as evidenced by the significant reduction of the Cu:Ce ratios shown in Table 1.

3.3 Thermal analysis

Table 2 summarizes the values of gravimetric and volumetric energy storage density. Experimental data were computed by integrating the DSC signal measured during the thermal analysis. The reported values are averaged over the different oxidation and reduction steps. Theoretical data were instead computed by referring to the theoretical reaction heat of the CuO to Cu_2O reduction, but accounting for the experimental values of Δm obtained. More in particular, the over-reduction of the samples was attributed to a higher content of CuO that reduces to Cu_2O, since the XRD/SEM analyses did not detect metallic copper or reduced ceria.
To compute the volumetric energy storage density, a bulk density of 2088 kg m^{-3} was used for all the samples. This was estimated by considering the theoretical density of Cu_2O, that is equal to 6000 kg m^{-3}, assuming a conservative value for the particle porosity of 40%, and a bed porosity of 42%.

The density value used should be conservative with respect to mixed Cu:Ce samples, due to the higher theoretical density of CeO_2 (i.e., ~7200 kg m^{-3}).

Table 2: Experimentally measured, and theoretically computed, values of energy storage density

Name	Experimental value		Theoretical value	
	[J g^{-1}]	[GJ m^{-3}]	[J g^{-1}]	[GJ m^{-3}]
Cu100	758	1.58	807	1.69
Cu70	552	1.15	650	1.36
Cu40	414	0.86	463	0.97
Cu0	–		–	

Data in Table 2 shows that the energy storage density is higher for the Cu100 sample and lower for the mixed oxides, as expected from the lower values of Δm observed in the thermogravimetric analyses. Experimental values are, on average, in good agreement with the theoretical ones, and about 12% lower, that is within the instrument accuracy. The volumetric values of energy storage density appear to be interesting when compared with other technologies. For instance, commercially used molten salts are characterized by an energy storage density of about 0.8 GJ m^{-3}, but the energy is stored as sensible heat and is released at lower temperature (290–565 °C), thus with subsequent lower efficiency in the thermodynamic cycle for energy generation. TCES systems relying on calcium carbonate calcination/carbonation (Karasavvas et al., 2018; Tregambi et al., 2021), among the most investigated in current literature, feature instead an energy storage density of about 0.75–1.75 GJ m^{-3} (Di Lauro et al., 2021), thus similar to that computed for the materials investigated in this study.

4. Conclusions

In this work different Cu:Ce mixed oxides were synthesized and tested under process conditions relevant for TCES applications, using a thermogravimetric analyzer with simultaneous thermal analysis. Tests were performed isothermally at 950°C, using N_2 as reactive gas during the reduction step and synthetic air as reactive gas during oxidation. All the samples underwent iterative reduction and oxidation, without any appreciable decay of reactivity over cycling. An over-reduction of the sample was observed with respect to nominal composition, which was partly attributed to a reduction of interfacial copper-ceria sites. Chemical-physical analyses on reduced samples revealed the only presence of Cu_2O and CeO_2, indicating that metallic copper is not formed or under detection limits of XRD, and potential CeO_2 reduction occurs without loosing the fluorite structure, under the process conditions investigated. SEM analyses showed that cerium migrated towards the surface after the four reaction cycles, as evidenced by the significant reduction of the Cu:Ce atomic ratios at the particles surface. The computed values of energy storage density range within 400–800 J g^{-1} and 0.9–1.7 GJ m^{-3} depending on the sample, and are comparable to those of other systems widely investigated in the literature. The preliminary results obtained in this work confirm that Cu:Ce mixed oxides may be interesting materials for TCES applications. Future studies will investigate the performance of these oxides under harsher reaction conditions, by performing also the reduction step in air at higher temperature, so as to avoid the need of a N_2 stream.

Acknowledgments

Mr. Luciano Cortese (STEMS-CNR) is gratefully acknowledged for his help in carrying out XRD and SEM-EDS analyses.

References

Alonso E., Pérez-Rábago C., Licurgo J., Fuentealba E., Estrada C.A., 2015, First experimental studies of solar redox reactions of copper oxides for thermochemical energy storage, Solar Energy, 115, 297−305.

Bareschino P., Mancusi E., Tregambi C., Pepe F., Urciuolo M., Brachi P., Ruppolo G., 2021, Integration of biomasses gasification and renewable-energies-driven water electrolysis for methane production, Energy, 230, 120863.

Block T., Schmücker M., 2016, Metal oxides for thermochemical energy storage: A comparison of several metal oxide systems, Solar Energy 126, 2016, 195−207.

Carrillo A.J., González-Aguilar J., Romero M., Coronado J.M., 2019, Solar Energy on Demand: A Review on High Temperature Thermochemical Heat Storage Systems and Materials, Chemical Reviews, 119, 4777−4816.

Chen C., Wang R., Shen P., Zhao D., Zhang N., 2015, Inverse CeO_2/CuO catalysts prepared from heterobimetallic metal-organic framework precursor for preferential CO oxidation in H_2-rich stream, International Journal of Hydrogen Energy, 40, 4830–4839.

Chen A., Yu X., Zhou Y., Miao S., Li Y., Kuld S., Sehested J., Liu J., Aoki T., Hong S., Farnesi Camellone M., Fabris S., Ning J., Jin C., Yang C., Nefedov A., Wöll C., Wang Y., Shen W., 2019, Structure of the catalytically active copper–ceria interfacial perimeter, Nature Catalysis, 2, 334–341.

Colussi S., Amoroso F., Katta L., Llorca J., Trovarelli A., 2014, The effect of ceria on the dynamics of CuO-Cu_2O redox transformation: CuO-Cu_2O hysteresis on ceria, Catalysis Letters., 144, 1023–1030.

De Vos Y., Jacobs M., Van Der Voort P., Van Driessche I., Snijkers F., Verberckmoes A., 2020, Development of Stable Oxygen Carrier Materials for Chemical Looping Processes—A Review, Catalysts, 10, 926.

Di Benedetto A., Landi G., Lisi L., 2017, CO reactive adsorption at low temperature over CuO/CeO_2 structured catalytic monolith, International Journal of Hydrogen Energy, 42, 12262–12275.

Di Lauro F., Tregambi C., Montagnaro F., Salatino P., Chirone R., Solimene R., 2021, Improving the performance of calcium looping for solar thermochemical energy storage and CO_2 capture, Fuel, 298, 120791.

Gigantino M., Brunser S.S., Steinfeld A., 2020, High-Temperature Thermochemical Heat Storage via the CuO/Cu_2O Redox Cycle: From Material Synthesis to Packed-Bed Reactor Engineering and Cyclic Operation, Energy & Fuels, 34, 16772−16782.

Hedayati A., Azad A.M., Rydén M., Leion H., Mattisson T., 2012, Evaluation of Novel Ceria-Supported Metal Oxides As Oxygen Carriers for Chemical-Looping Combustion, Industrial & Engineering Chemistry Research, 51, 12796−12806.

Imtiaz Q., Kurlov A., Rupp J.L.M., Müller C.R., 2015, Highly Efficient Oxygen-Storage Material with Intrinsic Coke Resistance for Chemical Looping Combustion-Based CO_2 Capture, ChemSusChem, 8, 2055–2065.

Imtiaz Q., Armutlulu A., Donat F., Naeem M.A., Müller C.R., 2021, Preventing Agglomeration of CuO-Based Oxygen Carriers for Chemical Looping Applications, ACS Sustainable Chemistry Engineering, 9, 5972–5980.

Karasavvas E., Panopoulos K.D., Papadopoulou S., Voutetakis S., 2018, Design of an Integrated CSP-Calcium Looping for Uninterrupted Power Production Through Energy Storage, Chemical Engineering Transactions, 70, 2131–2136.

Padula S., Tregambi C., Troiano M., Di Benedetto A., Salatino P., Landi G., Solimene R., 2022, Chemical Looping Reforming with Perovskite-Based Catalysts for Thermochemical Energy Storage, Energies, 15, 8556.

Popescu I., Piumetti M., Bensaid S., Marcu I.C., 2017, Study of Ce–Cu mixed oxide catalysts by in situ electrical conductivity measurements, Physical Chemistry Chemical Physics, 19, 31929–31939.

Portarapillo M., Aronne A., Di Benedetto A., Imparato C., Landi G., Luciani G., 2019, Syngas production through H_2O/CO_2 Thermochemical Splitting, Chemical Engineering Transactions, 74, 43–48.

Portarapillo M., Landi G., Luciani G., Imparato C., Vitiello G., Deorsola F.A., Aronne A., Di Benedetto A., 2022, Redox behavior of potassium doped and transition metal co-doped $Ce_{0.75}Zr_{0.25}O_2$ for thermochemical H_2O/CO_2 splitting, RSC Advances, 12, 14645–14654.

Rydén M., Jing D., Källén M., Leion H., Lyngfelt A., Mattisson T., 2014, CuO-Based Oxygen-Carrier Particles for Chemical-Looping with Oxygen Uncoupling − Experiments in Batch Reactor and in Continuous Operation, Industrial & Engineering Chemistry Research, 53, 6255–6267.

Szabová L., Skála T., Matolínová I., Fabris S., Farnesi Camellone M., Matolín V., 2013, Copper-ceria interaction: A combined photoemission and DFT study, Applied Surface Science, 267, 12–16.

Tregambi C., Bareschino P., Hanak D., Montagnaro F., Pepe F., Mancusi E., 2022, Modelling of an integrated process for atmospheric carbon dioxide capture and methanation, Journal of Cleaner Production, 356, 131827.

Tregambi C., Bareschino P., Mancusi E., Pepe F., Montagnaro F., Solimene R., Salatino P., 2021, Modelling of a concentrated solar power – photovoltaics hybrid plant for carbon dioxide capture and utilization via calcium looping and methanation, Energy Conversion and Management, 230, 113792.

Xiang D., Gu C., Xu H., Deng J., Zhu P., Xiao G., 2021, Al-Modified CuO/Cu2O for High-Temperature Thermochemical Energy Storage: from Reaction Performance to Modification Mechanism, ACS Applied Material & Interfaces, 13, 57274−57284.

Yilmaz D., Darwish E., Leion H., 2020, Thermochemical energy storage performance of copper oxides: Effect of support materials, Journal of Energy Storage, 32, 102012.